B-ANOMALIES: A MODEL BUILDER'S GUIDE

ADMIR GRELJO
PRISMA Cluster of Excellence and Mainz Institute for Theoretical Physics, Johannes Gutenberg-Universität Mainz, 55099 Mainz, Germany

I present a few model building lessons for high-p_T searches at the LHC when addressing recently reported hints on lepton flavour universality violation in semi-tauonic and rare B-meson decays.

1 Introduction

An increasing set of experimental measurements in semi-leptonic B-meson decays contradicts the SM predictions. Despite the fact that a compelling evidence for new physics (NP) is still missing, the case for it looks very encouraging as the coherent picture of deviations seems to be solidifying. B-anomalies consistently point towards a violation of lepton flavour universality (LFU) and are grouped into two different categories: (i) deviations from τ/ℓ (where $\ell = e, \mu$) universality in semi-tauonic decays as defined by $R(D^{(*)})$ observables ($b \to c\ell\nu$ charged currents) [1,2,3] and (ii) deviations from μ/e universality in rare decays as defined by $R(K^{(*)})$ observables ($b \to s\ell\ell$ neutral currents) [4,5]. Additional indication of consistent deviations in rare $b \to s\mu\mu$ transitions has been observed in the measurements of angular distributions of $B \to K^*\mu^+\mu^-$ [6,7]. The overall statistical significance of the discrepancies in the clean LFU observables alone is at the level of $4\,\sigma$ for both charged and neutral current processes [8,9,10,11,12].

While new experimental developments in B-decays are slowly approaching, it is important to provide consistent NP models to address present B-anomalies and predict smoking gun signatures in other (ongoing) searches, in particular, at the high-p_T frontier. Indeed, anomalies in B-meson decays point to a new mass scale potentially interesting for the ATLAS and CMS experiments. More precisely, the charged current anomaly ($b \to c\tau\nu$) implies the effective scale of $\mathcal{O}(1\,\text{TeV})$, while the neutral current anomaly ($b \to s\mu\mu$) implies the effective scale of $\mathcal{O}(30\,\text{TeV})$. The effective scale corresponds roughly to the mediator mass for $\mathcal{O}(1)$ couplings when the effect is tree-level generated. However, some explicit models exhibit parametric suppression (e.g. from flavour), or dynamical suppression (e.g. loop-generated), lowering the new mass scale towards the interesting range for the LHC. For example, a coherent picture of neutral and charged current B-anomalies is emerging when invoking i) a new (tree-level) dynamics at the TeV scale in (mainly) left-handed semi-leptonic currents such as $(\bar{Q}\gamma^\mu\sigma^a Q)(\bar{L}\gamma_\mu\sigma^a L)$, and ii) a flavour sym-

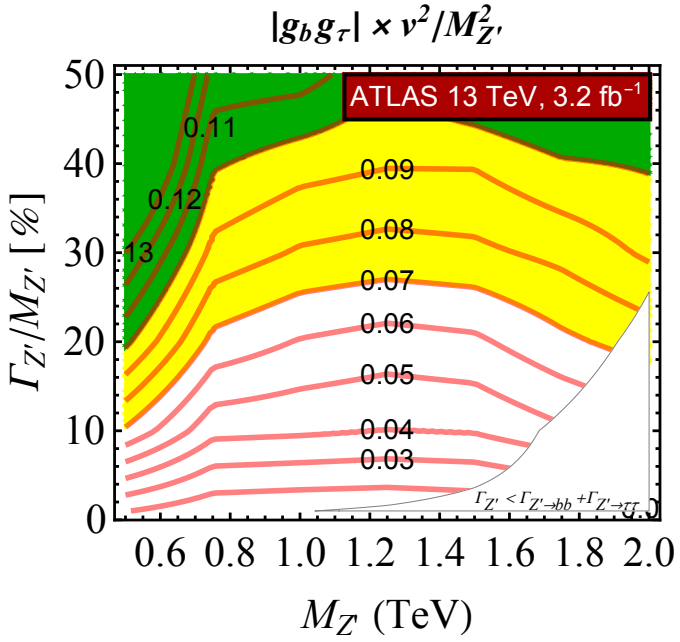

Figure 1 – LHC limits on the W' model for $R(D^{(*)})$ anomaly from $pp \to \tau^+\tau^-$. The plot is taken from the ref. [14].

metry implying dominant couplings are to the third family while the couplings to light families follow in a controlled way from the symmetry breaking spurions [16]. All tree-level models have either colour-neutral vectors (W' and Z') or colour-triplet scalar or vector leptoquarks (LQs), or combination of those.

The main purpose of this talk is to connect B-anomalies and high-p_T searches at the LHC. In the following, I will discuss a few model building lessons from refs. [13,14,15,16,17,18,19,20,21].

2 Semi-Tauonic B-decays and Di-Tau at high-p_T

The simplest way to generate the effective semi-leptonic triplet operator $(\bar{Q}\gamma^\mu\sigma^a Q)(\bar{L}\gamma_\mu\sigma^a L)$ at low-energies, and hence address the B-anomalies coherently, is to integrate at tree-level a massive colour-neutral real $\mathrm{SU}(2)_L$ triplet vector [13]. Let us take $W'^a \sim (W'^\pm, Z')$ coupled to the SM quarks and leptons as

$$\mathcal{L}_{W'} \supset \left(\lambda^q_{ij}\bar{Q}_i\gamma^\mu\sigma^a Q_j + \lambda^\ell_{ij}\bar{L}_i\gamma^\mu\sigma^a L_j\right) W'^{a\mu} \ . \tag{1}$$

We assume $\lambda^{q(\ell)}_{ij} \simeq g_{b(\tau)}\delta_{i3}\delta_{j3}$, such that the largest effects are in B-mesons and tau leptons, consistent with $U(2)$ flavour symmetry. Departures from this limit are constrained by low energy flavour data, including neutral meson mixing, rare B decays, LFU and LFV in τ decays and neutrino physics, a detail analysis of which has been performed in refs. [13,16].

An important constraint on the model is obtained from $pp \to \tau^+\tau^-$ search where a corresponding Z' is produced from the bottom fusion and decayed to a pair of tau leptons [14]. The resulting 95% CL upper limits on the $|g_b g_\tau| \times v^2/M^2_{Z'}$ as a function of the Z' mass and total Z' decay width, after recasting ATLAS 13 TeV $\tau^+\tau^-$ analysis with 3.2 fb^{-1} are shown in Fig. 1 with red isolines. These exclusions are to be compared with the preferred value from the fit to the $R(D^{(*)})$ anomaly, $|g_b g_\tau| \times v^2/M^2_{Z'} = (0.13 \pm 0.03)$, indicated in green ($1\sigma$) and yellow ($2\sigma$) shaded regions in the plot. Note that these results do not depend on the specific assumptions about extra Z' decay channels. The main conclusion here is that the explanation of the $R(D^{(*)})$ anomaly can only be reconciled with the existing LHC $\tau^+\tau^-$ searches for a relatively wide resonance where the model's parameter space is approaching the strongly coupled regime such that perturbative calculations start to fail.

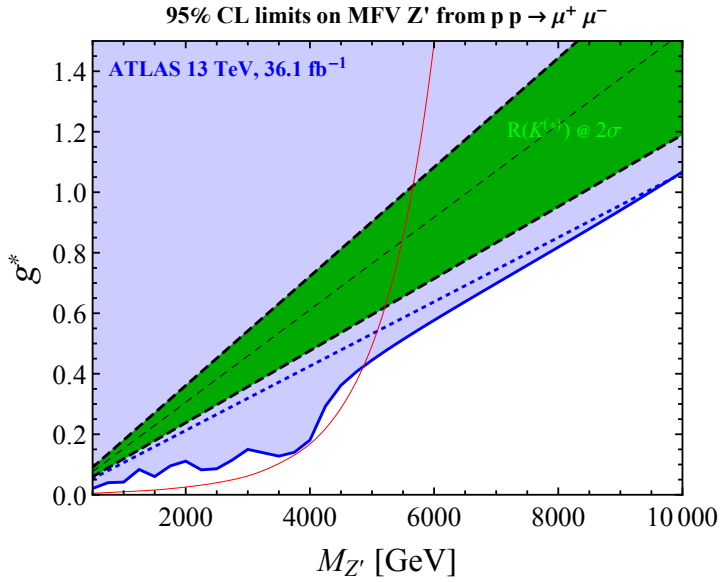

Figure 2 – LHC limits on the MFV Z' model for $R(K^{(*)})$ from $pp \to \mu^+\mu^-$. The plot is taken from the ref. [15].

To circumvent this problem, in ref. [20], we considered the case in which the $R(D^{(*)})$ anomaly is generated by the $b \to c\tau\bar{N}_R$ transition mediated instead by an $SU(2)_L$ singlet W', where N_R is a light right-handed neutrino. This is in contrast to the triplet model of ref. [13], which requires the $W'^{\pm}$ to be nearly degenerate with the corresponding Z', and the flavour structures of $W'^{\pm}$ and Z' couplings to be related through the CKM mixing matrix. These requirements are lifted in the singlet model such that the stringent $\tau^+\tau^-$ limits are satisfied.

3 Rare B-decays and High-p_T dilepton tails

Recent hints on lepton flavour universality violation in $b \to s\mu\mu$ transitions suggest new physics in $pp \to \mu^+\mu^-$ process at the LHC. Even if the new mass scale is well beyond the kinematical reach for on-shell production, the signal in the high-p_T dilepton tail might still be observed as first noted in ref. [15].

To illustrate this point, we assume a Z' vector boson model, $\mathcal{L} \supset g_Q^{(1),ij}(\bar{Q}_i\gamma^\mu Q_j)Z'_\mu + g_L^{(1),kl}(\bar{L}_k\gamma^\mu L_l)Z'_\mu$, with $g_Q^{(1),ii} = g_L^{(1),22} = g^*$ where $i = 1, 2, 3$ and MFV structure in the quark sector $g_Q^{(1),23} = V_{ts}g^*$, as dictated by the neutral meson oscillation constraints. We derive limits on g^* as a function of the mass $M_{Z'}$, fitting the dimuon invariant mass spectrum from the ATLAS $\mu^+\mu^-$ search at 13 TeV with 36.1 fb^{-1} of data. (The Z' decay width is determined by decays into the SM fermions, $\Gamma_{Z'}/M_{Z'} \approx 5g_*^2/(6\pi)$.)

The results are shown in Fig. 2. The limits in the full model are shown with solid-blue while those in the EFT are shown with dashed-blue. We see that for a mass $M_{Z'} > 5$ TeV, the EFT limit works quite well. On top of this, we show with green band the best fit and 2σ interval which reproduces the $b \to s\mu\mu$ flavour anomalies, showing how LHC dimuon searches already exclude such a scenario independently of the Z' mass. The red solid line indicates the naive bound obtained when interpreting the limits on the narrow-width resonance production, $\sigma(pp \to Z') \times \mathcal{B}(Z' \to \mu^+\mu^-)$.

4 Consistency of the low-p_T data and single mediator models

The consistency of the B-anomalies with other low-p_T data, such as (other) rare B decays, LFU and LFV in τ decays and Z-boson decays, has been investigated in ref. [16] starting with the left-handed semi-leptonic operators within the SM EFT. The complete set of single-mediator

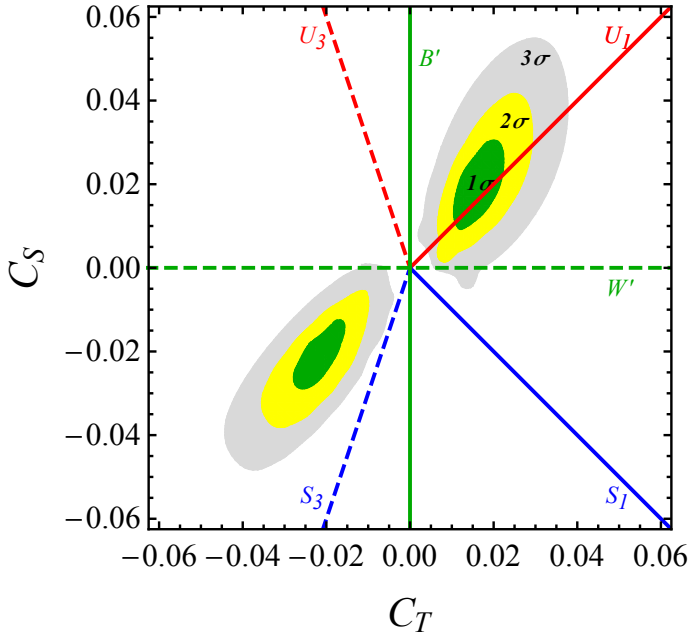

Figure 3 – Coherent picture of B-anomalies and single-mediator models. The plot is taken from the ref. [16].

models with tree-level matching to the vector triplet and/or singlet $V-A$ semi-leptonic operators consists of: colour-singlet vectors $B'_\mu \sim (\mathbf{1},\mathbf{1},0)$ and $W'_\mu \sim (\mathbf{1},\mathbf{3},0)$, colour-triplet scalars $S_1 \sim (\bar{\mathbf{3}},\mathbf{1},1/3)$ and $S_3 \sim (\bar{\mathbf{3}},\mathbf{3},1/3)$, and vectors $U_1^\mu \sim (\mathbf{3},\mathbf{1},2/3)$ and $U_3^\mu \sim (\mathbf{3},\mathbf{3},2/3)$ [21]. (The quantum numbers in brackets indicate colour, weak, and hypercharge representations, respectively.)

In Fig. 3 we show the correlation between triplet and singlet operators predicted in all single-mediator models, compared to the regions favoured by the EFT fit from ref. [16]. A remarkably simple explanation of all the low-energy data is obtained by supplementing the SM with a single field – vector leptoquark representation $U_1^\mu \sim (\mathbf{3},\mathbf{1},2/3)$. Importantly, leptoquarks induce semi-leptonic transitions at tree level, while pure 4-quark and 4-lepton transitions arise only at one loop[21]. The exceptional feature of this particular representation is the absence of tree-level down-quark-to-neutrino, as well as up-quark-to-charged-lepton transitions, naturally suppressing (a set of) otherwise strongly constrained observables. The first explicit ultraviolet completion of this simplified model is provided in [17].

5 B-anomalies inspired leptoquarks

The B-anomalies inspired LQ searches at the LHC exhibit an interplay between three production mechanisms: LQ pair production, single LQ production in association with the lepton, and di-lepton production (see e.g. [18] for a recent discussion). Interestingly enough, the three production mechanisms scale differently with the size of the LQ-q-ℓ coupling and consequently offer complementary probes of the LQ parameter space.

To illustrate this point, in Fig. 4 we show what values of Yukawa couplings one needs to use to have equality between the total inclusive single LQ production cross section and the total inclusive LQ pair production cross section for a given initial quark flavour as a function of the LQ mass. This plot clearly shows the importance of the single LQ production in the heavy LQ regime. In addition, for the $R(D^{(*)})$ anomaly, one expects LQ-b-τ coupling of $\mathcal{O}(1)$ for a TeV scale LQ which is in the right ballpark. The calculation leading to Fig. 4 is performed using the Monte Carlo tool for LQ and NLO in QCD presented in ref. [18].

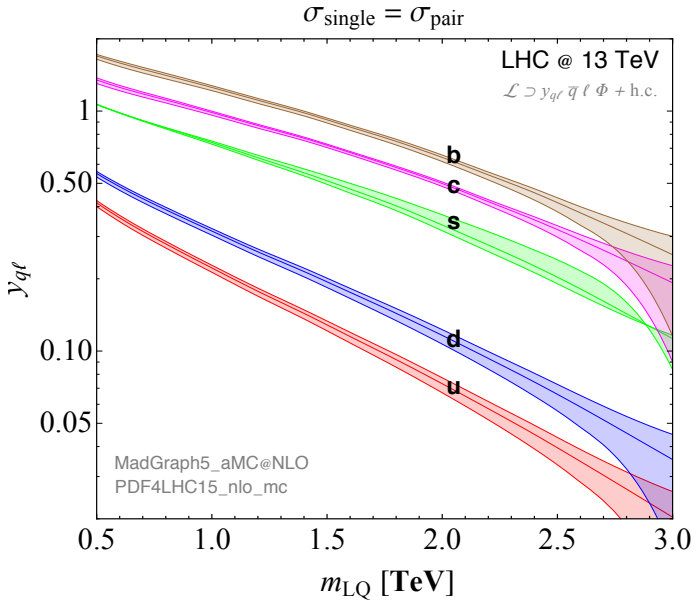

Figure 4 – LQ pair production versus single LQ plus lepton production at the LHC. The plot is taken from the ref. [18].

Acknowledgments

I thank organisers for the invitation to present this talk. I am also grateful to my collaborators [13,14,15,16,17,18,19,20,21].

References

1. J. P. Lees *et al.* [BaBar Collaboration], Phys. Rev. D **88**, no. 7, 072012 (2013) doi:10.1103/PhysRevD.88.072012 [arXiv:1303.0571 [hep-ex]].
2. S. Hirose *et al.* [Belle Collaboration], Phys. Rev. Lett. **118**, no. 21, 211801 (2017) doi:10.1103/PhysRevLett.118.211801 [arXiv:1612.00529 [hep-ex]].
3. R. Aaij *et al.* [LHCb Collaboration], Phys. Rev. Lett. **115**, no. 11, 111803 (2015) Erratum: [Phys. Rev. Lett. **115**, no. 15, 159901 (2015)] doi:10.1103/PhysRevLett.115.159901, 10.1103/PhysRevLett.115.111803 [arXiv:1506.08614 [hep-ex]].
4. R. Aaij *et al.* [LHCb Collaboration], Phys. Rev. Lett. **113**, 151601 (2014) doi:10.1103/PhysRevLett.113.151601 [arXiv:1406.6482 [hep-ex]].
5. R. Aaij *et al.* [LHCb Collaboration], JHEP **1708**, 055 (2017) doi:10.1007/JHEP08(2017)055 [arXiv:1705.05802 [hep-ex]].
6. R. Aaij *et al.* [LHCb Collaboration], Phys. Rev. Lett. **111**, 191801 (2013) doi:10.1103/PhysRevLett.111.191801 [arXiv:1308.1707 [hep-ex]].
7. R. Aaij *et al.* [LHCb Collaboration], JHEP **1602**, 104 (2016) doi:10.1007/JHEP02(2016)104 [arXiv:1512.04442 [hep-ex]].
8. B. Capdevila, A. Crivellin, S. Descotes-Genon, J. Matias and J. Virto, JHEP **1801**, 093 (2018) doi:10.1007/JHEP01(2018)093 [arXiv:1704.05340 [hep-ph]].
9. W. Altmannshofer, P. Stangl and D. M. Straub, Phys. Rev. D **96**, no. 5, 055008 (2017) doi:10.1103/PhysRevD.96.055008 [arXiv:1704.05435 [hep-ph]].
10. L. S. Geng, B. Grinstein, S. Jger, J. Martin Camalich, X. L. Ren and R. X. Shi, Phys. Rev. D **96**, no. 9, 093006 (2017) doi:10.1103/PhysRevD.96.093006 [arXiv:1704.05446 [hep-ph]].
11. Y. Amhis *et al.* [HFLAV Collaboration], Eur. Phys. J. C **77**, no. 12, 895 (2017) doi:10.1140/epjc/s10052-017-5058-4 [arXiv:1612.07233 [hep-ex]].
12. G. D'Amico, M. Nardecchia, P. Panci, F. Sannino, A. Strumia, R. Torre and A. Urbano,

JHEP **1709**, 010 (2017) doi:10.1007/JHEP09(2017)010 [arXiv:1704.05438 [hep-ph]].
13. A. Greljo, G. Isidori and D. Marzocca, JHEP **1507** (2015) 142 doi:10.1007/JHEP07(2015)142 [arXiv:1506.01705 [hep-ph]].
14. D. A. Faroughy, A. Greljo and J. F. Kamenik, Phys. Lett. B **764** (2017) 126 doi:10.1016/j.physletb.2016.11.011 [arXiv:1609.07138 [hep-ph]].
15. A. Greljo and D. Marzocca, Eur. Phys. J. C **77** (2017) no.8, 548 doi:10.1140/epjc/s10052-017-5119-8 [arXiv:1704.09015 [hep-ph]].
16. D. Buttazzo, A. Greljo, G. Isidori and D. Marzocca, JHEP **1711** (2017) 044 doi:10.1007/JHEP11(2017)044 [arXiv:1706.07808 [hep-ph]].
17. L. Di Luzio, A. Greljo and M. Nardecchia, Phys. Rev. D **96** (2017) no.11, 115011 doi:10.1103/PhysRevD.96.115011 [arXiv:1708.08450 [hep-ph]].
18. I. Dorsner and A. Greljo, arXiv:1801.07641 [hep-ph].
19. A. Greljo and B. A. Stefanek, Phys. Lett. B **782** (2018) 131 doi:10.1016/j.physletb.2018.05.033 [arXiv:1802.04274 [hep-ph]].
20. A. Greljo, D. J. Robinson, B. Shakya and J. Zupan, arXiv:1804.04642 [hep-ph].
21. I. Dorsner, S. Fajfer, A. Greljo, J. F. Kamenik and N. Konik, Phys. Rept. **641** (2016) 1 doi:10.1016/j.physrep.2016.06.001 [arXiv:1603.04993 [hep-ph]].